Progress In Electromagnetics Research C, Vol. 41, 163–174, 2013

DESIGN OF A COMPACT WIDEBAND MIMO ANTENNA FOR MOBILE TERMINALS

Xing-Xing Xia, Qing-Xin Chu*, and Jian-Feng Li

School of Electronic and Information Engineering, South China University of Technology, Guangzhou, Guangdong 510640, China

Abstract—A new broadband multiple-input multiple-output (MIMO) antenna with good isolation and compact size is proposed. The proposed antenna consists of two G-shaped elements in the upper layer and two inverted L protrude branches and a T slot etched in ground which is used to reduce the mutual coupling. This planar antenna has a bandwidth of 100% with $|S_{11}| \leq -10\,\text{dB}$ from 2.26 to 6.78 GHz. The value of isolation between the two antenna elements is more than 22.5 dB in the whole band. The experimental results verify the simulations.

1. INTRODUCTION

MULTIPLE-INPUT MULTIPLE-OUTPUT (MIMO) technology has been reported for several years, which significantly enhances the performance of wireless communication systems [1, 2]. One important requirement for MIMO antenna systems is the need for good isolation between antenna elements. In some applications, such as cellular communication, MIMO technology is easy to be implemented at the base station where antenna elements separate many wavelengths, and good isolation is easily available. However, in mobile terminals, reaching high isolation in small size is difficult to fulfill.

Various methods have been devised to improve isolation between the elements of a narrowband MIMO antenna, e.g., [3–12]. In [3, 4], good isolation is achieved by adding parasitic elements, which can create a reverse coupling to reduce mutual coupling. However, the method of adding parasitic elements is sensitive to the position of the parasitic elements. A neutralization line is inserted between two PIFAs in [5, 6]. This method can introduce some current on the neutralization

Received 21 April 2013, Accepted 22 June 2013, Scheduled 2 July 2013
* Corresponding author: Qing-Xin Chu (qxchu@scut.edu.cn).

line and create an additional electromagnetic field to enhance port-to-port isolation. But it is a challenge to find a low impedance area that suits for the neutralization line. In addition, the use of electromagnetic band-gap (EBG) is able to suppress surface wave propagation [7, 8], and thus improve the isolation between radiating elements. However, this method occupies significant areas. Other isolation enhanced techniques, such as incorporating a protruded ground between the antennas [9, 10], inserting slits into the ground [11], applying multi-port conjugate (MC) match [12], are also used. Nowadays, broadband and Ultra-wideband (UWB) MIMO antenna represents a very appealing solution for multi-standard device because of the increasing number of operating frequency bands required in mobile terminals. There are several effective methods used in narrowband, which also suit for broadband or UWB to improve isolation, such as adding stub or branch [13–16] and etching slot in the ground [17–19]. Though the method of adding branch has good isolation, it acquires antenna size. Though the method of etching slot is not complicated, it affects the integrity of antenna ground. As to reaching high isolation in all the broadband or UWB, it is an open issue.

In this paper, a compact wideband planar diversity antenna for mobile terminals covering LTE 2300/2600, WLAN 2.4/5.2/5.8-GHz, and the lower UWB band (3.1–4.8 GHz) is proposed. The antenna can act as 4G, Wifi, UWB MIMO antenna with largely cut size and cost. It has a bandwidth of 100% with $|S_{11}| \leq -10$ dB from 2.26 to 6.78 GHz. We use the method combining adding ground branches and etching slot in the ground to improve isolation. The isolation between the two antenna elements is larger than 22.5 dB in the whole band (about 25 dB in the most of the band). The paper is organized as follows: In Section 2, the design of the antenna with inverted L branches and T-slot is introduced. In Section 3, the working mechanism of the MIMO antenna is investigated to show how to form the broadband. Current distributions are shown to demonstrate the isolation, and the effects of some important parameters of the proposed antenna are also discussed. In Section 4, simulated and measured radiation gain patterns are given, and MEG, radiation efficiency, correlation coefficient are also calculated. Finally, a conclusion is given in Section 5.

2. ANTENNA CONFIGURATION

The geometry of the proposed MIMO antenna system is shown in Fig. 1. The values of l_1, l_2, l_3, l_4 are 2.7 mm, 4.5 mm, 5.1 mm, 13 mm, respectively. The design of the antenna is based on a FR-4 substrate with dimensions $55 \times 50 \times 0.8\,\text{mm}^3$ and relative permittivity 4.4. The

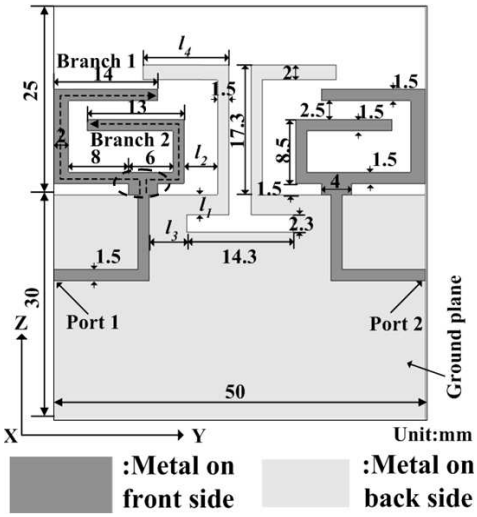

Figure 1. Detailed dimension of the proposed antenna.

MIMO antenna consists of two G-shaped symmetric face-to-face dual-branch monopoles printed on the upper part of the substrate. Each monopole occupies a surface of $17.5 \times 13.5\,\text{mm}^2$. In order to increase the isolation between two monopoles, two inverted L-shaped ground branches and a small T-shaped slot are etched in the ground.

3. EXPERIMENTAL RESULTS AND DISCUSSIONS

The antenna has been simulated using Ansoft simulation software HFSS v13. To verify the performance of the wideband MIMO antenna, a prototype has been fabricated (see Fig. 2) and measured. The simulated and measured S-parameters are shown in Fig. 3. It is observed that the $|S_{11}|$ and $|S_{21}|$ curves of overall trend between simulated and measured results are almost well matched except that the measured $|S_{11}|$ shifts a litter higher than the simulated one. This is due to factors such as imperfection fabrication and measurement tolerances. It can be seen from Fig. 3 that the two-branch antenna generates three resonant modes around 2.5, 4.7 and 5.3 GHz. In addition, the $|S_{21}|$ is smaller than -20 dB.

The summarized design procedure for the MIMO antenna can be formulated into the following steps:

1) Design a single antenna element that has a broadband feature. Our idea is based on integrating several close frequency resonant modes

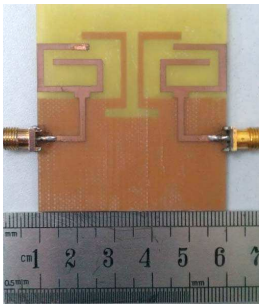

Figure 2. Prototype of the proposed antenna.

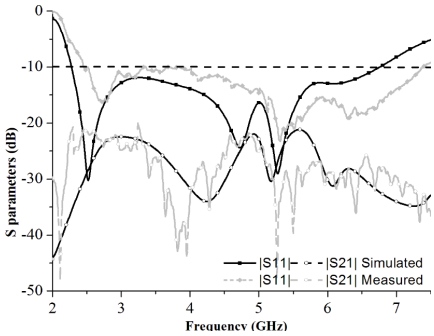

Figure 3. Simulated and measured S-parameters of the proposed MIMO antenna.

which can form broadband. The important issue is to design the lengths of branch 1 and branch 2, which directly determine whether the broadband feature can be formed or not.

2) Utilize ground branches to improve isolation in low band tentatively. It is difficult to improve isolation in low band, so we consider low-band propriety. The main thing is to determine the position of the inverted L branches that little affect the $|S_{11}|$ when adding these two branches. So the gap, between the antenna element and branch (l_2), and the length of horizontal length of the branch (l_4) need to be carefully considered.

3) Improve high band isolation by etching a T slot in the ground. The novel idea is that part of the T-slot is formed by two ground branches and the combination of these two improving isolation methods. The horizontal length of the slot is designed near $\lambda_0/2$ at 6.0 GHz.

As depicted in Fig. 1, we design a single dual-branch monopole antenna that has a convention ground. It has two branches and forms a G-shape. The length of branch 1 is 40 mm and branch 2 28 mm. From the formulation [20] that calculates the $\lambda_0/2$ resonant mode of a monopole antenna:

$$f = \frac{c}{\sqrt{\varepsilon} \cdot 2l}, \quad \varepsilon = \frac{\varepsilon_r + 1}{2} \tag{1}$$

where c is the speed of light in vacuum, ε_r the dielectric of the substrate, and l the length of the resonator. We can calculate the $\lambda_0/2$ resonant modes of branch 1 and branch 2, which are 2.28 GHz, 3.26 GHz, respectively. Fig. 4 shows simulated reflect coefficients of the single dual-branch monopole antenna, branch 1 and branch 2,

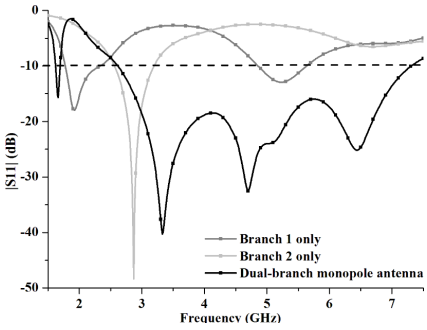

Figure 4. Simulated reflect coefficients of the dual-branch monopole antenna, branch 1 only and branch 2 only.

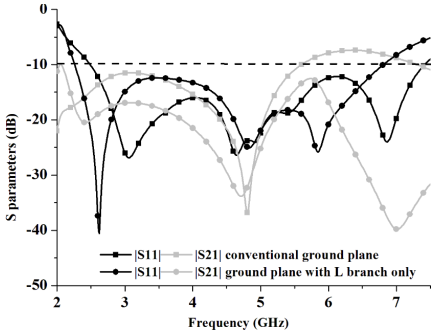

Figure 5. Simulated S-parameters of the conventional ground plane and ground plane with dual inverted L branch only.

respectively. According Fig. 4, it can be observed that branch 1 and branch 2 can produce a $\lambda_0/2$ resonant mode at 1.9 GHz and a $\lambda_0/2$ resonant mode at 2.84 GHz, respectively. The simulated resonant mode results appear a little lower than the calculated ones. This can be explained by that the physical antenna has a stub added in the end branch signed as dotted oval in Fig. 1, which acts as a match stub and also as a open shunt stub that makes the resonance lower.

A wide operating band with $|S_{11}| \leq -10$ dB extending from 2.6 to 7.4 GHz and another lower narrow band around 1.7 GHz are produced when two branches are arranged face to face. The two branches should not be too close because strong coupling can deteriorate antenna performance, so we set it 2.5 mm. It can be noticed that original branch 1 resonant mode at 1.9 GHz shifts low while original branch 2 resonant mode at 2.87 GHz shifts high when the two branches arrange together. Besides, two more new higher frequency resonant modes are formed. The antenna presented in [13] has a similar broadband formed mechanism which uses the method that makes several resonant modes arranged closely. We neglect the lower narrow-band around 1.7 GHz because of no practical use in this narrow band.

We can form a MIMO antenna by using two symmetric antenna elements without decoupling process. From Fig. 5, the isolation of the conventional ground plane is bad except at 4.6 GHz. Through surveying the left picture of current distribution at 4.6 GHz in Fig. 6(b), it can be noticed that the current concentrates between the left-bottom part of branch 1 and the up-verge of ground, which seem like a slot antenna. When the length of the "slot antenna" is 10 mm ($1/4\lambda_0$ at

4.6 GHz), it can resonate at 4.6 GHz. So the current cannot flow to the other antenna, and high isolation can be formed without decoupling method at 4.6 GHz. Firstly, we try to use ground branch method that is widely utilized to improve isolation between the two antennas. Two inverted L branches are added extending from the ground and can be as two reflectors that reflect the space wave back. The designed length of each inverted L-branch is 30.3 mm which is between the lengths of branch 1 (40 mm) and branch 2 (28 mm), so it can work between these two $\lambda_0/2$ resonant modes. We can find in Fig. 5 that it can simply improve the isolation in low band, but there is little influence in high band. Secondly, in order to improve the isolation in the high band, we additionally introduce a T-shape slot etched in the ground. The length of horizontal slot is 14.3 mm and can trap ground wave around 6.3 GHz (calculated from (1)). Simulated and measured results have been shown in Fig. 3. In short, with the combination of inverted L-branches and T-slots, the isolation in the whole band especially high band is significantly improved.

Figure 6 shows current distribution of the conventional ground MIMO antenna and proposed MIMO antenna at 2.5 GHz, 4.6 GHz, 6.0 GHz, respectively. As demonstrated in Fig. 6(a), the current is mainly reflected by the left side inverted L-branch near the excited antenna and blocked by the T-slot at 2.5 GHz. The other part of the

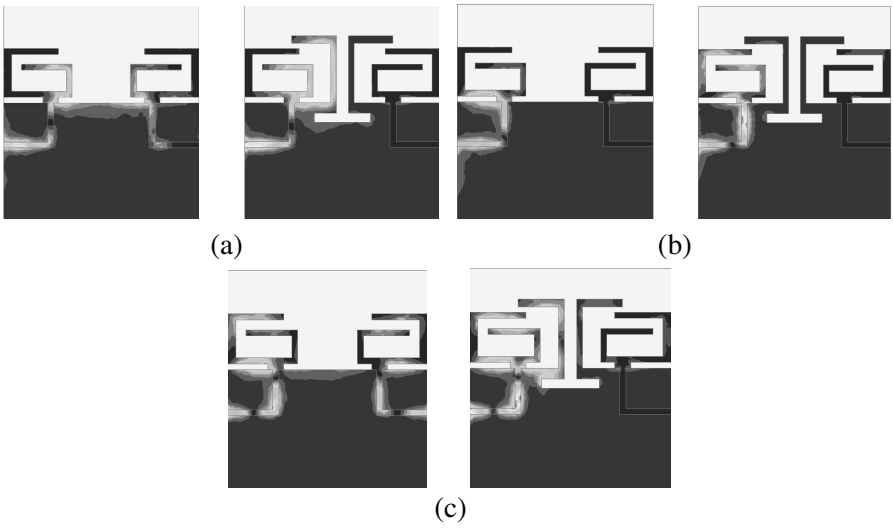

Figure 6. Current distribution of the conventional ground MIMO antenna and proposed MIMO antenna. (a) 2.5 GHz, (b) 4.6 GHz, (c) 6.0 GHz.

inverted L branch has nearly no current flowing or coupling on it in spite of the distance between the two inverted L-branches nearly 0.025 λ_0 at 2.5 GHz. In Fig. 6(b), both of the inverted L-branches and T-slot have little current for there is no current flowing to the other antenna at 4.6 GHz. In Fig. 6(c), we can see that the surface current also concentrates between the left-side L-branch and the excited antenna. Because the horizontal length of the T-slot is 14.3 mm (shorter than $\lambda_0/2$ at 6.0 GHz), and then the slot can trap the current with the combination of L inverted-branch at 6.0 GHz.

From the result of the proposed antenna with decoupling structure, it can be seen that the decoupling structure has great effect on improving isolation. Our aim is to investigate the influence to the isolation and make a better understanding of the decoupling structure. The study is based on the analysis of l_1, l_2, l_3, l_4 given in Fig. 1. In Fig. 7, we can observe that l_1 has little influence on the lower band, but it can improve $|S_{11}|$ at high band. As to $|S_{21}|$, it can decrease the isolation as l_1 decreases. This can be explained by that when l_1 decreases, the branch comes closer to the antenna, then the coupling is increased.

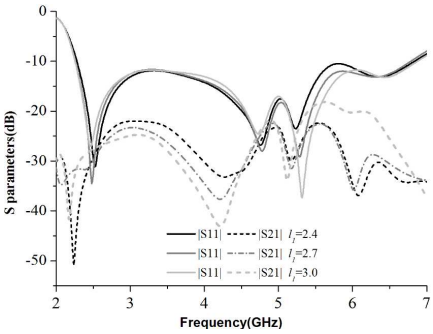

Figure 7. S-parameters against frequency with different l_1.

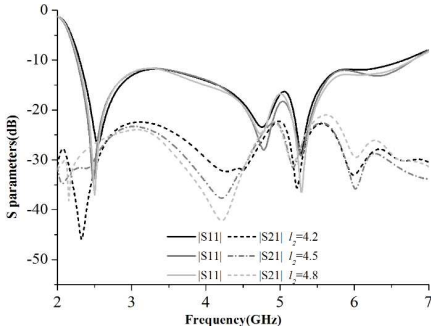

Figure 8. S-parameters against frequency with different l_2.

It can be seen in Fig. 8 that l_2 has little influence on $|S_{11}|$, but the isolation will be improved with the increase of l_2. Because it can be clearly seen that with the increase of l_2, the distance between the antenna and decoupled branch becomes larger.

In Fig. 9, we use l_3 to adjust the match in high band. The length of slot can influence the impedance of the ground. As we can see, the $|S_{11}|$ becomes better with the increase of l_3.

In Fig. 10, we can observe that l_4 has a great influence on the $|S_{11}|$ and isolation. With the change of l_4, $|S_{11}|$ becomes definitely different.

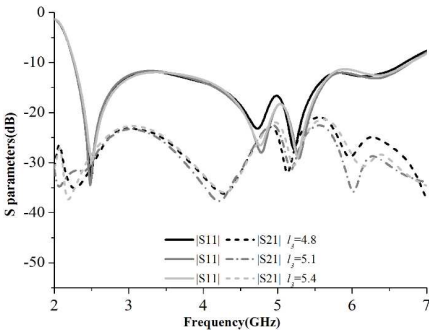

Figure 9. S-parameters against frequency with different l_3.

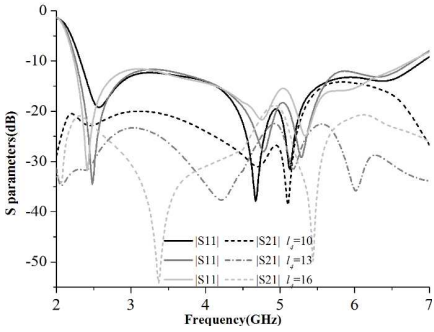

Figure 10. S-parameters against frequency with different l_4.

This can be explained by that l_4 has a great influence on the couple between the antenna and the branch. As l_4 becomes larger, the couple becomes stronger, and the isolation becomes weaker.

From these figures it can be concluded that l_1, l_4 have more effect on resonant frequency thanl_2, l_3. As to $|S_{21}|$, l_2, l_4 have more effect on isolation than l_1, l_3. In addition, l_4 needs more consideration.

4. DIVERSITY PERFORMANCE OF THE PROPOSED MIMO ANTENNA

The simulated and measured radiation gain patterns of the MIMO antenna with monopole1 excited (port 1 excited and port 2 terminated with a 50-Ω load) at 4.5 GHz are shown in Fig. 11, and the gains have been normalized.

It can be observed in Fig. 11 that the simulated and measured radiation gain patterns at 4.5 GHz agree well. The discrepancy between the measured and simulated results comes principally from our measurement setup such as angle calibration which causes the deviation between measured and simulated phi in x-y plane. Moreover, in small antenna measurements, it is usually difficult to efficiently choke the feeding cables to avoid currents flowing on their outer part, and these cables are very difficult to maintain perfectly parallel to the length of the PCB due to the size and the proximity of the ferrite chokes [13].

We choose to calculate the mean effective gain (MEG) and relation coefficient ρ in our antenna system. MEGs are calculated based on the series of the assumption defined in [21, 22], and the calculated MEGs at 2.5, 4.0 and 6.0 GHz are shown in Table 1. The radiation, total

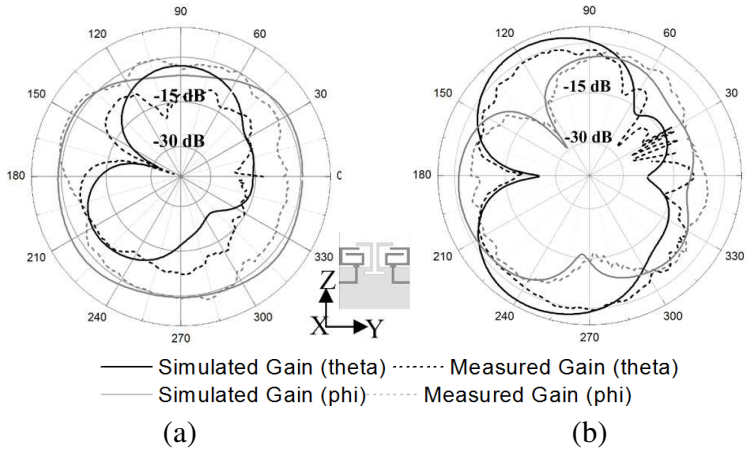

Figure 11. Simulated and measured radiation gain patterns at 4.5 GHz. (a) x-y plane, (b) x-z plane.

Table 1. Diversity performance of the prototype of the proposed antenna.

f (GHz)	MEG_1 (dB)	MEG_2 (dB)	$\lvert\mathrm{MEG}_1/\mathrm{MEG}_2\rvert$ (dB)	η_1 (%)	η_2 (%)	$\rho_{12} \approx \rho_{21}$	Gain (dB)
2.5	−3.29	−3.28	0.01	93.9	93.8	0.0006	3.51
4.0	−3.40	−3.41	0.01	95.3	94.7	0.0075	2.35
6.0	−3.89	−3.90	0.01	86.9	86.6	0.0059	2.83

efficiencies and gain are also listed in Table 1. For isotropic/uniform signal propagation environments, the correlation coefficient ρ and envelope correlation coefficient ρ_e can be calculated by [22–24]:

$$|\rho_{ij}|^2 = \rho_{eij} = \left| \frac{\left| S_{ii}^* S_{ij} + S_{ji}^* S_{jj} \right|}{\left| \left(1 - |S_{ii}|^2 - |S_{ji}|^2\right)\left(1 - |S_{jj}|^2 - |S_{ij}|^2\right) \eta_{radi}\eta_{radj} \right|^{1/2}} \right|^2 \quad (2)$$

where η_{radi} is the ith antenna radiation efficiency and can be obtained from HFSS simulation results.

From Table 1 we know that ρ is smaller than 0.1 and the radiation efficiency larger than 85% which meet the demand of all the broadband with high efficiency and low coefficient. It can be observed that the proposed antenna can easily fulfill the diversity criteria: $\rho_{e12} < 0.5$ and $|\mathrm{MEG}_1/\mathrm{MEG}_2| < 3\,\mathrm{dB}$ [25], assuming that the mean incident power on each antenna is the same, the equality criterion between P_i and P_j reduces to equality between MEG_i and MEG_j.

5. CONCLUSION

In this paper, a new broadband method has been proposed to enhance the isolation of two closely spaced G-shaped antennas. The combination of the inverted L-branch and T-slot etched in ground reduces the mutual coupling significantly. The results show that the isolation in the operation band is lower than -22.5 dB. Several parameters have been studied on the effect on $|S_{11}|$, $|S_{21}|$. Besides, l_4 needs carefully designed. The envelop correlation coefficient and MEGs of the antenna elements have been calculated to evaluate the diversity performance of the proposed MIMO antenna. The results show that the antenna is suitable for the application in wireless communication.

ACKNOWLEDGMENT

This work was supported by the National Natural Science Foundation of China (61171029) and Guangzhou Science and Technology Project (12C42081659).

REFERENCES

1. Foschini, Jr., G. J., "Layered space-time architecture for wireless communication in a fading environment when using multi-element antennas," *Bell Labs Tech. J.*, 41–59, 1996.
2. Foschini, Jr., G. J. and M. J. Gans, "On limits of wireless communication in a fading environment when using multiple antennas," *Wireless Personal Commun.*, Vol. 6, 311–335, 1998.
3. Li, Z., Z. Du, M. Takahashi, K. Saito, and K. Ito, "Reducing mutual coupling of MIMO antennas with parasitic elements for mobile terminals," *IEEE Trans. on Antennas and Propag.*, Vol. 60, 473–481, 2012.
4. Addaci, R., A. Diallo, C. Luxey, P. L. Thuc, and R. Staraj, "Dual-band WLAN diversity antenna system with high port-to-port isolation," *IEEE Antennas Wireless Propag. Lett.*, Vol. 11, 244–247, 2012.
5. Diallo, A., C. Luxey, P. L. Thuc, T. Staraj, and G. Kossiavas, "Study and reduction of the mutual coupling between two mobile phone PIFAs operating in the DCS1800 and UMTS bands," *IEEE Trans. on Antennas and Propag.*, Vol. 54, 3063–3073, 2006.
6. Li, J. F. and Q. X. Chu, "Compact conventional phone antenna integrated with wideband multiple-input-multiple-output antenna," *Microw. Opt. Technol. Lett.*, Vol. 54, 1958–1962, 2012.

7. Sievenpiper, D., L. Zhang, R. F. J. Broas, N. G. Alexopolous, and E. Yablonovitch, "High-impedance electromagnetic surfaces with a forbidden frequency band," *IEEE Microw. Theory Tech.*, Vol. 47, 2059–2074, 1999.
8. Yang, F. and Y. Rahmat-Samii, "Microstrip antennas integrated with electromagnetic band-gap (EBG) structures: A low mutual coupling design for array applications," *IEEE Trans. on Antennas and Propag.*, Vol. 51, 2936–2946, 2003.
9. Chi, G., L. Binhong, and D. Qi, "Dual-band printed diversity antenna for 2.4/5.2-GHz WLAN application," *Microw. Opt. Technol. Lett.*, Vol. 45, 561–563, 2005.
10. Ding, Y., Z. Du, K. Gong, and Z. Feng, "A novel dual-band printed diversity antenna for mobile terminals," *IEEE Trans. on Antennas and Propag.*, Vol. 55, 2088–2096, 2007.
11. Ayatollahi, M., Q. Rao, and D. Wang, "A compact, high isolation and wide bandwidth antenna array for long term evolution wireless devices," *IEEE Trans. on Antennas and Propag.*, Vol. 45, 601–602, 2012.
12. Bhatti, R. A., S. Y. Yi, and S. O. Park, "Compact antenna array with port decoupling for LTE-standardized mobile phones," *IEEE Antennas Wireless Propag. Lett.*, Vol. 8, 1430–1433, 2009.
13. Li, J. F., Q. X. Chu, and T. G. Huang, "A compact wideband MIMO antenna with two novel bent slits," *IEEE Trans. on Antennas and Propag.*, Vol. 60, 482–489, 2012.
14. Najam, A. I., Y. Duroc, and S. Tedjni, "UWB-MIMO antenna with novel stub structure," *Progress In Electromagnetics Research C*, Vol. 19, 245–257, 2011.
15. Zhou, F., Z. P. Qian, T. T. Liu, J. W. Han, and C. Peng, "Design of diversity antenna for ultra-wideband applications," *2010 IEEE International Conference on Ultra-Wideband (ICUWB)*, Vol. 1, 1–4, 2010.
16. Zhang, S., Z. N. Ying, J. Xiong, and S. L. He, "Ultrawideband MIMO/diversity antennas with a tree-like structure to enhance wideband isolation," *IEEE Antennas Wireless Propag. Lett.*, Vol. 8, 1279–1282, 2009.
17. Zhou, X., X. Quan, and R. L. Li, "A dual-broadband MIMO antenna system for GSM/UMTS/LTE and WLAN handsets," *IEEE Antennas Wireless Propag. Lett.*, Vol. 11, 551–554, 2012.
18. Liu, L., H. Zhao, T. S. P. See, and Z. N. Chen, "A printed ultra-wideband diversity antenna," *Proc. IEEE International Conference on Ultra-Wideband*, 351–356, 2006.

19. Kim, I., C. W. Jung, Y. Kim, and Y. Kim, "Low-profile wideband MIMO antenna with suppressing mutual coupling between two antennas," *Microw. Opt. Technol. Lett.*, Vol. 50, 1336–1339, 2008.
20. Waldschmidt, C. and W. Wiesbeck, "Compact wide-band multimode antennas for MIMO and diversity," *IEEE Trans. on Antennas and Propag.*, Vol. 52, 458–462, 2004.
21. Karaboikis, M. P., V. C. Papamichael, G. F. Tsachtsiris, C. F. Soras, and V. T. Makios, "Integrating compact printed antennas onto small diversity/MIMO terminals," *IEEE Trans. on Antennas and Propag.*, Vol. 56, 2067–2078, 2008.
22. Blanch, S., J. Romeu, and I. Corbella, "Exact representation of antenna system diversity performance from input parameter description," *IEEE Electron. Lett.*, Vol. 39, 705–707, 2003.
23. Taga, T., "Analysis for mean effective gain for mobile in land mobile radio environments," *IEEE Trans. on Veh. Technol.*, Vol. 39, 117–131, 1990.
24. Blanch, S., J. Romeu, and I. Corbella, "Exact representation of antenna system diversity performance from input parameter description," *IEEE Electron. Lett.*, Vol. 39, 705–707, 2003.
25. Aughan, R. G. V. and J. B. Andersen, "Antenna diversity in mobile communications," *IEEE Trans. on Veh. Technol.*, Vol. 36, 147–172, 1987.